



Sodium butyrate inhibits activation of ROS/NF- κ B/NLRP3 signaling pathway and angiogenesis in human retinal microvascular endothelial cells

Xin Cao · Yue Di · Ya-jing Tian · Xiao-bo Huang · Yue Zhou · Dong-mei Zhang · Yu Song

Received: 25 April 2024 / Accepted: 22 February 2025
© The Author(s), under exclusive licence to Springer Nature B.V. 2025

Abstract

Background To determine the impact of sodium butyrate on the activation of the reactive oxygen species (ROS)/nuclear factor kappa B (NF- κ B)/NLR family pyrin domain containing 3 (NLRP3) signaling pathway and angiogenesis in human retinal microvascular endothelial cells (HRMECs) caused by high glucose (HG).

Methods HRMECs were grown for 24 h or 72 h in HG solution (30 mmol/L D-glucose) with 5 mM NaB. Using Cell Counting Kit-8, the effects of HG and NaB levels on the viability of HRMECs were examined. Using various kits, intracellular ROS levels, lactate dehydrogenase (LDH), and Malondialdehyde (MDA) in cell supernatants were measured. Western blot, Immunofluorescence, and Real-time quantitative polymerase chain reaction were employed to quantify protein and messenger RNA expression. Using wound-healing and tube formation tests, the migratory proficiency and angiogenesis of HRMECs were evaluated.

Results NaB demonstrated a reduction in ROS production, as well as the release of LDH and MDA in HG-induced HRMECs. Additionally, NaB led to a

decrease in protein expression of phosphorylation of NF- κ B, NLRP3, Caspase 1, interleukin, vascular cell adhesion molecule-1 and intercellular adhesion molecule-1. The impact of HG on zonula occluden-1, a tight junction protein, was attenuated by NaB. Furthermore, NaB inhibited the migration and tube formation of HRMECs partly by ROS/NF- κ B/NLRP3 pathway.

Conclusion NaB suppresses the activation of ROS/NF- κ B/NLRP3 signaling pathway and angiogenesis in HRMECs induced by HG.

Keywords Sodium butyrate · Nuclear factor kappa B · NLRP3 · Angiogenesis · Human retinal microvascular endothelial cells

Abbreviations

NaB	Sodium butyrate
HRMECs	Human retinal microvascular endothelial cells
HG	High glucose
NF- κ B	Nuclear factor kappa B
ROS	Reactive oxygen species
NLRP3	NLR family pyrin domain containing 3
CCK-8	Cell Counting Kit-8
LDH	Lactate dehydrogenase
MDA	Malondialdehyde
IF	Immunofluorescence
RT-qPCR	Real-time quantitative polymerase chain reaction
mRNA	Messenger RNA

X. Cao · Y. Di · Y. Tian · X. Huang · Y. Zhou · D. Zhang · Y. Song (✉)
Department of Ophthalmology, The Second
Affiliated Hospital of Nantong University, No. 666,
Shengli Road, Nantong 226001, Jiangsu Province,
People's Republic of China
e-mail: songyu2387@163.com

IL-1 β	Interleukin-1 β
VCAM-1	Vascular cell adhesion molecule-1
ICAM-1	Intercellular adhesion molecule-1
ZO-1	Zonula occluden-1
TJ	Tight junction
DM	Diabetes mellitus
DR	Diabetic retinopathy
PDR	Proliferative diabetic retinopathy
SOX4	SRY (sex determining region Y)-box 4
TXNIP	Thioredoxin-interacting protein
HDACs	Histone deacetylases
T1DM	Type 1 diabetes mellitus
VEGFR2	Vascular endothelial growth factor receptor2
T2DM	Type 2 diabetes mellitus
BRB	Blood retina barrier
GPCRs	G-protein coupled receptors
oxLDL	Oxidized low-density lipoprotein
JAMs	Junctional adhesion molecules
NAC	N-Acetylcysteine
GSH	Glutathione
TMAO	Trimethylamine N-oxide
TMA	Trimethylamine

Introduction

Diabetes mellitus (DM) comprises a collection of chronic metabolic disorders primarily arising from inadequate absolute or relative insulin secretion, or impaired utilization of insulin. Currently, the global count of adults afflicted by diabetes is estimated to be around 463 million in 2019. It is predicted that this number could escalate to 700 million by the year 2045 [29]. Diabetic retinopathy (DR) is a progressive retinal microvascular ailment intricately linked with prolonged periods of hyperglycemia. About 75% of patients with the diabetic course over 15 years suffer from DR. After 25 years of diabetes, 20% of these DR patients will be affected by proliferative diabetic retinopathy (PDR), which seriously threatens eyesight [2]. The pathogenesis of DR is characterized by HG-induced sterile inflammation, oxidative stress, and visible microvascular alterations, such as abnormal permeability, retinal ischemia–reperfusion injury, neovascularization, and macular edema. Current treatment of DR includes retinal photocoagulation, vitrectomy, and anti-VEGF therapy. Still, these methods mainly delay the progression of DR and cannot

improve the patient's visual function, and there are many limitations and iatrogenic complications [16]. There is an urgent need for a novel and effective therapeutic approach to decelerate the advancement of DR.

Persistent oxidative stress and chronic low inflammation mutually promote endothelial dysfunction, which critically initiates the progression of diabetic microvascular damage [20]. Elevated levels of reactive oxygen species (ROS) can result in damage to retinal endothelial cells, heightened microvascular permeability, and attraction of inflammatory cells to the site of inflammation [26]. The nuclear factor kappa B (NF- κ B) plays a pivotal role in triggering various inflammatory factors and has been demonstrated to be involved in endothelial dysfunction and angiogenesis. Gu et al. found that SRY (sex determining region Y)-box 4 (SOX4) enhances inflammation and angiogenesis in retinal endothelial cells through the activation of the NF- κ B signaling pathway [34]. Another key player, the NLR family pyrin domain containing 3 (NLRP3) inflammasome, represents a group of intracellular innate immune proteins and sensors that react to the stimulation of pathogen- and damage-associated molecular patterns. It has also been observed that disturbances in glucose levels serve as a pivotal trigger, setting off a cascade of heightened sterile inflammatory reactions driven by the NLRP3 inflammasome [19]. Recent research found that the ROS/thioredoxin-interacting protein (TXNIP)/NLRP3 axis was involved in the enhanced retinal microvascular permeability and apoptosis caused by HG levels in diabetics [4]. Sodium butyrate (NaB) is a fatty acid derivative that is common in foods that are part of the daily diet. Additionally, NaB is produced in considerable quantities by the gut microbiota in the colon via the fermentation of indigestible dietary fibre [14]. Butyrate functions as an endogenous inhibitor of histone deacetylases (HDACs), leading to increased histone acetylation the rate of and reduced electrostatic repulsion between DNA and histone proteins. As a result, the chromatin structure becomes more relaxed, causing alterations in the gene expression profile [6]. Notably, butyrate's anti-inflammatory effects have been attributed to its ability to inhibit the activation of the NLRP3 inflammasome through the redox signaling pathway [33, 39]. Recent studies have unveiled the therapeutic potential of NaB in addressing metabolic disorders. To reduce metabolic stress,

for instance, researchers found that NaB inhibited inflammatory reactions in the digestive tract. According to Khan and Jena, NaB has been suggested to potentially reduce plasma glucose levels in mice with type 1 diabetes mellitus (T1DM) by modulating the p38/ERK MAPK pathway [12]. Moreover, Chen et al. demonstrated that NaB may block neovascularization by blocking the TNXIP/vascular endothelial growth factor receptor2 (VEGFR2) pathway [36].

Indeed, it appears that NaB's antioxidant, anti-inflammatory, and neovascularization suppressing properties may be responsible for the positive impacts it has on tissues. However, the specific effect of NaB on the behavior of HRMECs in type 2 diabetes mellitus (T2DM) remains poorly understood. Therefore, the primary objective of our study was to investigate how NaB influences the ROS/NF- κ B/NLRP3 signaling pathway and angiogenesis in HRMECs exposed to HG.

Materials and methods

Cell culture

HRMECs were sourced from Procell (Wuhan, China, CP-H130) and cultured in Endothelial cell medium (ECM, ScienCell, 1001) supplemented with 10% fetal bovine serum (Gibco, 10099141C) and 100 U/ml streptomycin/penicillin (10,000 U/ml, Gibco, 15,140,148) at a temperature of 37 °C under a controlled environment of 5% CO₂ and 95% ambient air. The HRMECs were categorized into different groups as administrated by: D-glucose (Sigma, 50–99-7), NaB (Sigma, 156-54-7), mannose (Sigma, 3458-28-4), N-Acetylcysteine (Sigma, 38,520-57-9) and Trimethylamine N-oxide (Sigma, 1184-78-7). The HRMECs used were at 3–5 passage numbers to ensure consistency and reproducibility of the experimental results.

Cell viability assay

The viability and growth of HRMECs were evaluated using the Cell Counting Kit-8 (CCK-8, Biosharp, BS350A). In a nutshell, HRMECs were seeded at a density of 2×10^3 per well in a 96-well plate and allowed to adhere for 24 h. Subsequently, the cells were cultured in serum-free medium for a duration of

12 h to stimulate cell growth. After 72 h, one group was subjected to stimulation with varying concentrations of D-glucose (0, 5.5, 15, 30 mM) and 5.5 mM Mannose, while another group was treated with NaB at concentrations of 0, 1, 5, and 10 mM. Following this, 10 μ l of CCK-8 solution was added to each well, and the plates were further incubated at 37 °C for 2 to 4 h. We next checked the absorbance at 450 nm. At least 3 sets of experiments were conducted.

Western blot assay

Cell lysates were prepared by combining RIPA lysis buffer (Beyotime, P0013B), PMSF (Beyotime, ST505) and a phosphatase inhibitor cocktail (Beyotime, P1082) to extract total proteins. The protein concentrations in the cell lysates were measured using a BCA protein assay kit (Beyotime, P0010). Samples were subjected to sodium dodecyl sulfate–polyacrylamide gel electrophoresis (SDS-PAGE) with gel densities ranging from 5 to 14% for separation. After blocking with 5% nonfat milk for 2 h, the PVDF membranes (Millipore, ISEQ00010) were incubated overnight with antibodies against p65 (Proteintech, 80,979-1-RR, 1:1000), p-p65 (Proteintech, 82,335-1-RR, 1:1000), caspase-1 (Proteintech, 81,482-1-RR, 1:1000), IL-1 β (Proteintech, 66,737-1-Ig, 1:1000), NLRP3 (Abcam, ab263899, 1:1000), ICAM-1 (Proteintech, 15,364-1-AP, 1:1000), VCAM-1 (Proteintech, 66,294-1-Ig, 1:1000), ZO-1 (Proteintech, 66,452-1-Ig, 1:1000). Subsequently, the membranes were washed three times with TBST and then incubated with secondary antibodies (Proteintech, SA00001-1 and SA00001-2) for 2 h at room temperature. Relative glutamate dehydrogenase (GAPDH, Proteintech, 60,004-1-Ig, 1:5000) used as an internal control.

RNA extraction and real-time quantitative PCR (RT-qPCR)

According to the manufacturer's instructions, total RNA was extracted from HRMECs using TRIzol reagent (Invitrogen, 15,596,026). The isolated RNA was then reverse transcribed into complementary DNA using PrimeScript RT Master Mix (Takara, RR036A). RT-qPCR was performed utilizing TB Green Premix Ex Taq (Takara, RR820A). The primer sequences for PCR amplifications were sourced from Primer Bank

(<https://pga.mgh.harvard.edu/primerbank/>) and synthesized by Qingke Biotechnology (Beijing, China). The specific primer sequences are provided in the table below:

Gene Name	Sequence (5'–3')
NLRP3	Forward: CGTGAGTCCCATTAAAGATGGAGT Reverse: CCCGACAGTGGATATAGAACAGA
Caspase1	Forward: TTTCCGCAAGGTTTCGATTTTCA Reverse: GGCATCTGCGCTCTACCATC
IL-1 β	Forward: ATGATGGCTTATTACAGTGGCAA Reverse: GTCGGAGATTCGTAGCTGGA

Immunofluorescence (IF)

HRMECs were fixed in freshly produced 4% para-formaldehyde (Byotime, P0099) at 4 °C for 30 min. Following this, the cells were washed three times with PBS for 10 min each wash. To block non-specific binding, the cells were blocked with 1% BSA (Biosharp, BS114) in PBS for 1 h at room temperature. Subsequently, the samples were subjected to three PBS washes before being exposed to ZO-1 antibody (Proteintech, 66,452-1-Ig, 1:100) at 4°C and a relative humidity of 70% overnight. After three PBS washes, the cells were treated with secondary antibodies conjugated with Alexa Fluor 488 (Abcam, ab150077, 1:500) for 1 h at 37 °C in a humidified dark room. The cell nuclei were stained using 4', 6-diamidino-2-phenylindole (DAPI, Sigma, D9542). The fluorescence images were captured using a confocal microscope (Nikon, Tokyo, Japan).

Tube formation

Cells were plated onto a Matrigel-coated 96-well plate at a density of 2×10^5 cells per well (Corning, 354,230). Following a 12-h incubation at 37 °C, various media conditions were introduced to the plate, including NG (5.5 mM D-glucose), HG (30 mM D-glucose), NG with NaB (5.5 mM D-glucose + 5 mM NaB) or HG with NaB (30 mM D-glucose + 5 mM NaB). After that, an inverted microscope was used to take pictures of the tubes. The number of branch points within the tube network was quantified using Image J software.

Scratch test

Cells were evenly distributed in 6-well plates at a density of 2×10^5 cells per well. Following a 12-h period of serum deprivation in FBS-free ECM, the cells were subjected to a scratch using a 1 mL pipette tip, rinsed with PBS, and stimulated at 37 °C for 72 h with different media. Scratches were photographed at 0 and 24 h to demonstrate cell confluence. Using ImageJ software, the average widths of the scratch wounds were quantified. The migration distance was determined by calculating the difference between the scratch width at 24 h and its width at 0 h.

Measurement of ROS production

The fluorescent probe 2', 7'-dichlorofluorescein diacetate (H2DCF-DA, obtained from Med Chem Express, HY-D0940) was employed to measure intracellular levels of ROS. This probe is sensitive to oxidation and undergoes a transformation when exposed to ROS, resulting in the production of a visible compound known as DCF. To evaluate intracellular ROS levels, cells were treated with a concentration of 10 μ M H2DCF-DA in the culture medium for a duration of 30 min at a temperature of 37 °C. Subsequently, images were captured using a fluorescence microscope, and the acquired images were quantitatively analyzed utilizing ImageJ software.

Maleic dialdehyde assay (MDA)

The amount of MDA was measured by using commercial detection kits from the Jiancheng Institute of Biotechnology in Nanjing, China (A003-1–2). The obtained results were analyzed in accordance with the guidelines provided by the manufacturer of the kits.

Cell cytotoxicity (LDH) test

After subjecting HRMECs to a 72-h treatment with NaB (5 mM), the culture supernatants were carefully transferred to a new 96-well plate. The plate was then placed in a dark environment at room temperature and allowed to incubate for 30 min. The measurement of absorbance was carried out using a micro-plate reader, with excitation set at 450 nm. The

Cytotoxicity LDH Assay Kit utilized for this purpose was obtained from Med Chem Express, with the catalog number HY-K1090.

Statistical analysis

The experiments were repeated three times to ensure statistical significance (SD). Statistical analyses were conducted using Graphpad Prism, version 8.0 (Graphpad Software, San Diego, CA, USA). To assess the presence of statistically significant differences among the groups, one-way analysis of variance (ANOVA) followed by Bonferroni's multiple comparison test was employed. Two-sided P-values were used, with significance considered at $P < 0.05$.

Results

High concentrations of NaB have a harmful effect on HRMECs viability

Firstly, we found no significant difference in cell viability between the control group (none-glucose) and the mannose group compared to the NG group (normal-glucose). However, when the glucose concentration was increased to 15, 30, and 50 mM, we observed a significant increase in cell viability in the HG group compared to the NG group (Fig. 1A). Based on this result, we intervened with cells using 30 mM glucose in subsequent experiments [15].

Subsequently, we found that post-intervention with 1 and 5 mM NaB showed no significant change in cell viability compared to the control group, but cell viability significantly decreased after intervention with 10 mM NaB, suggesting that a high concentration of NaB can inhibit the activity of HRMECs (Fig. 1B). Therefore, the concentration of NaB used in subsequent experiments was 5 mM.

NaB suppressed the oxidative stress induced by HG in HRMECs

The HG-stimulated group exhibited significantly higher ROS levels compared to the NG group (Fig. 2A and B). And increased MDA generation and LDH release due to enhanced cell damage were also seen after HG administration (Fig. 2C and D). All above adverse alterations were considerably decreased by 5 mM NaB treatment.

NaB decreased the activation of NF- κ B/NLRP3 inflammasome pathway and upregulation of VCAM-1 and ICAM-1 induced by HG in HRMECs

The NF- κ B/NLRP3 inflammasome pathway was activated by HG compared to the NG group, as evidenced by the increased protein expression of p65 phosphorylation (Fig. 3 and B), mRNA and protein expression of NLRP3 (Fig. 3C, D and E), Caspase1 (Fig. 3C, D and F) and IL-1 β (Fig. 3C, D and G) after 30 mM glucose incubation for 72 h. And 5 mM

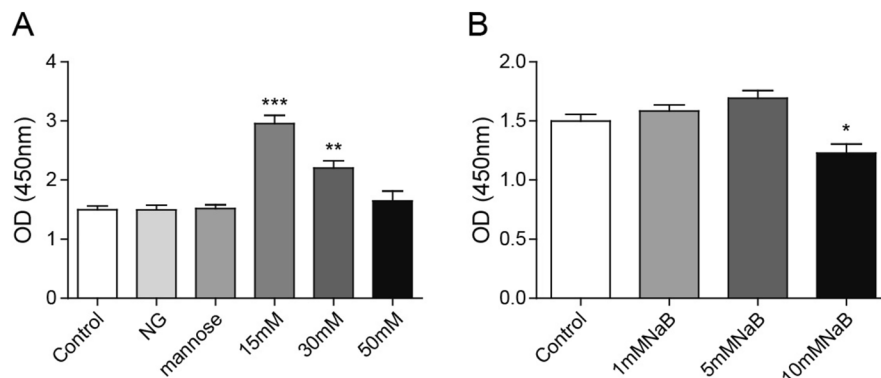


Fig. 1 Effects of glucose or NaB at different concentrations on HRMECs viability. Groups: (1) Control: no D-glucose; (2) NG: 5.5 mM D-glucose; (3) Mannose: 5.5 mM mannose; (4) 15 mM: 15 mM D-glucose; (5) 30 mM: 30mMD-glucose; (6) 50 mM: 50 mM D-glucose. **A** Cell viability of HRMECs

when no D-glucose, 5.5 mM mannose, 5.5, 15-, 30-, and 50-mM D-glucose. **B** Cell viability of HRMECs when NaB at 0, 1, 5, and 10 mM with no D-glucose. NG, normal glucose, 5.5 mM; * $P < 0.05$; ** $P < 0.01$; *** $P < 0.001$. Each experiment was repeated at least three times

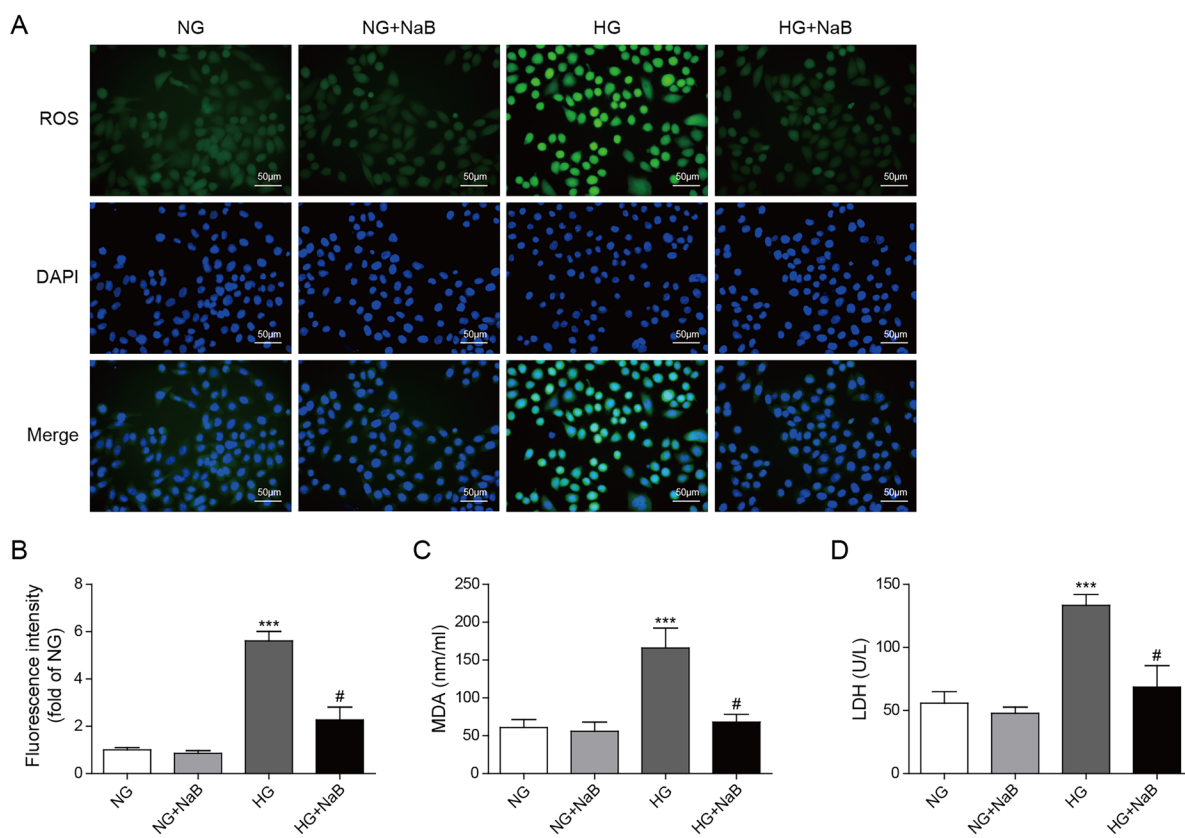


Fig. 2 ROS level, MDA and LDH production affected by glucose and NaB in HRMECs. Groups: (1) NG: 5.5 mM D-glucose; (2) NG + NaB: 5.5 mM D-glucose + 5 mM NaB; (3) HG: 30 mM D-glucose; (4) HG + NaB: 30 mM D-glucose + 5 mM NaB. **A** H2DCF-DA of ROS level in HRMECs (green fluorescence). **B** Quantitative analysis of the fluorescence intensity that represents intracellular ROS levels.

C MDA levels in HRMECs after NG, NG + NaB, HG, HG + NaB administration for 72 h. **D** LDH levels in HRMECs after NG, NG + NaB, HG, HG + NaB administration for 72 h. * $P < 0.05$ and *** $P < 0.001$ compared with the NG group; # $P < 0.05$ compared with the HG group. Each experiment was repeated at least three times

NaB treated cells in a HG medium decreased these alterations. Simultaneously, the protein expression of VCAM-1 and ICAM-1 significantly increased after being cultured in HG media for 72 h in HRMECs, but the treatment of 5 mM NaB reversed these changes (Fig. 3H and I).

NaB protected the impaired barrier function induced by HG in HRMECs

Increased endothelial permeability is often attributed to zonula occludens-1 (ZO-1) down regulation. HG stimulation led to a significant reduction in the protein expression of ZO-1 at cell junctions in endothelial cell monolayers, a phenomenon that was reversed by 5 mM NaB (Fig. 4A and B). IF staining

demonstrated that HG decreases the protein expression of ZO-1, while NaB successfully prevented this effect (Fig. 4C).

NaB reduced the migration and tube formation stimulation induced by HG in HRMECs

In vitro scratch assays were employed to assess the influence of NaB on cell migration. The number of migrating cells was markedly increased following HG treatment, whereas it was significantly attenuated by treatment with 5 mM NaB (Fig. 5A and C). Also, the tube formation data showed that HRMECs had more branching points after being exposed to HG, but less after being exposed to NaB (Fig. 5B and D).

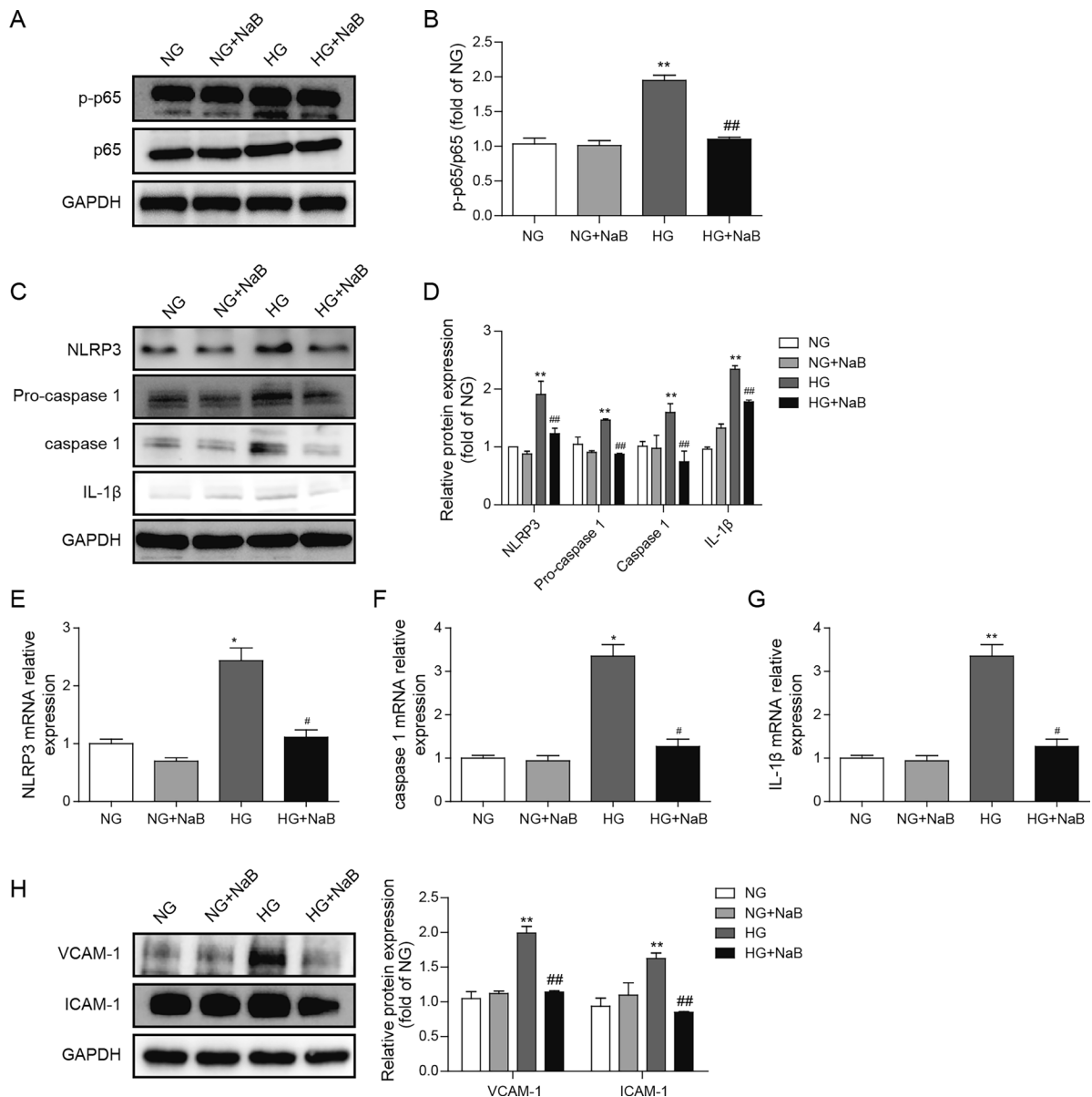


Fig. 3 NF- κ B/NLRP3 inflammasome pathway activation level, VCAM-1 and ICAM-1 expression level affected by glucose and NaB in HRMECs. Groups: (1) NG: normal glucose, 5.5 mM D-glucose; (2) NG+NaB: 5.5 mM D-glucose + 5 mM NaB; (3) HG: 30 mM D-glucose; (4) HG+NaB: 30 mM D-glucose + 5 mM NaB. **A** p-p65 and p65 protein expression in HRMECs after NG, NG+NaB, HG, HG+NaB administration for 72 h. **B** Quantitative analysis of the gray value of Western blot that represents p-p65/p65 protein expression. **C** NLRP3, Pro-caspase1, Caspase1 and IL-1 β protein expression in HRMECs after NG, NG+NaB, HG, HG+NaB administration for 72 h. **D** Quantitative analysis of the gray value of Western blot that represents NLRP3, Pro-caspase1, Caspase1

and IL-1 β protein expression. **E** NLRP3 mRNA expression in HRMECs after NG, NG+NaB, HG, HG+NaB administration for 72 h. **F** Caspase1 mRNA expression in HRMECs after NG, NG+NaB, HG, HG+NaB administration for 72 h. **G** IL-1 β mRNA expression in HRMECs after NG, NG+NaB, HG, HG+NaB administration for 72 h. **H** VCAM-1 and ICAM-1 protein expression in HRMECs after NG, NG+NaB, HG, HG+NaB administration for 72 h. **I** Quantitative analysis of the gray value of Western blot that represent VCAM-1 and ICAM-1 protein expression. * $P < 0.05$ and ** $P < 0.01$ compared with the NG group; # $P < 0.05$ and ## $P < 0.01$ compared with the HG group. Each experiment was repeated at least three times

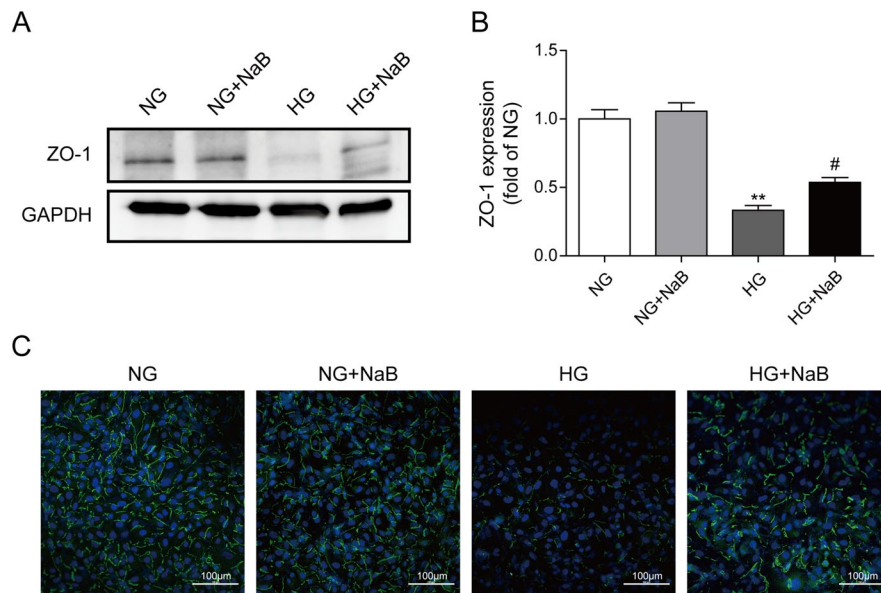


Fig. 4 ZO-1 expression affected by glucose and NaB in HRMECs. Groups: (1) NG: normal glucose, 5.5 mM D-glucose; (2) NG+NaB: 5.5 mM D-glucose + 5 mM NaB; (3) HG: 30 mM D-glucose; (4) HG+NaB: 30 mM D-glucose + 5 mM NaB. **A** ZO-1 protein expression in HRMECs after NG, NG+NaB, HG, HG+NaB administration for 72 h. **B** Quantitative analysis of the gray value of western blot that repre-

sents ZO-1 protein expression. **C** ZO-1 protein expression in HRMECs after NG, NG+NaB, HG, HG+NaB administration for 72 h detected by IF (ZO-1 stained by green fluorescence, nucleus stained by DAPI). ** $P < 0.01$ compared with the NG group; # $P < 0.05$ compared with the HG group. Each experiment was repeated at least three times

NaB inhibited HG-induced activation of ROS/NF- κ B/NLRP3 pathway and angiogenesis in HRMECs

Through immunofluorescence assays, we discovered that the ROS inhibitors N-Acetylcysteine (NAC) and NaB both suppressed the HG-induced ROS increase. Simultaneously, the ROS activator Trimethylamine N-oxide (TMAO) reversed NaB's inhibitory effect on ROS (Fig. 6A). Similarly, both NAC and NaB suppressed HG-induced oxidative stress and cell damage, and TMAO reversed NaB's inhibitory effect (Fig. 6B). Additionally, via Western blot analysis, we found that NAC and NaB inhibited the activation of the HG-induced NF- κ B/NLRP3 signaling pathway and the downstream expression of caspase-1 and IL-1 β , while TMAO reversed NaB's inhibitory effect (Fig. 6C). Finally, through cell scratch and angiogenesis experiments, we observed that both NAC and NaB inhibited HG-induced migration and angiogenesis in HRMECs, and TMAO ameliorated NaB's inhibitory effect on cell migration and angiogenesis (Fig. 6D and E).

Discussion

DR stands as a primary contributor to vision impairment and blindness. However, a genuine remedy capable of retarding the advancement of DR is still conspicuously absent [25]. NaB possesses anti-inflammatory, anti-angiogenesis, and antioxidant qualities that help to reduce the generation of pro-inflammatory cytokines while increasing the expression of antioxidant enzymes [5], which has been studied as treatment or prevention in inflammatory bowel disease [22], colorectal cancer [18], brain damages [13], liver injury [17], et al. However, its involvement in the pathophysiology of DR is unknown. Our study demonstrated that NaB administration could inhibit NF- κ B/NLRP3 inflammatory activation and oxidative stress induced by HG in HRMECs. And NaB could prevent HRMECs migration and tube formation by suppressing the activation of the ROS/NF- κ B/NLRP3 pathway induced by HG. Therefore, our research outcomes have unveiled that NaB holds significant promise

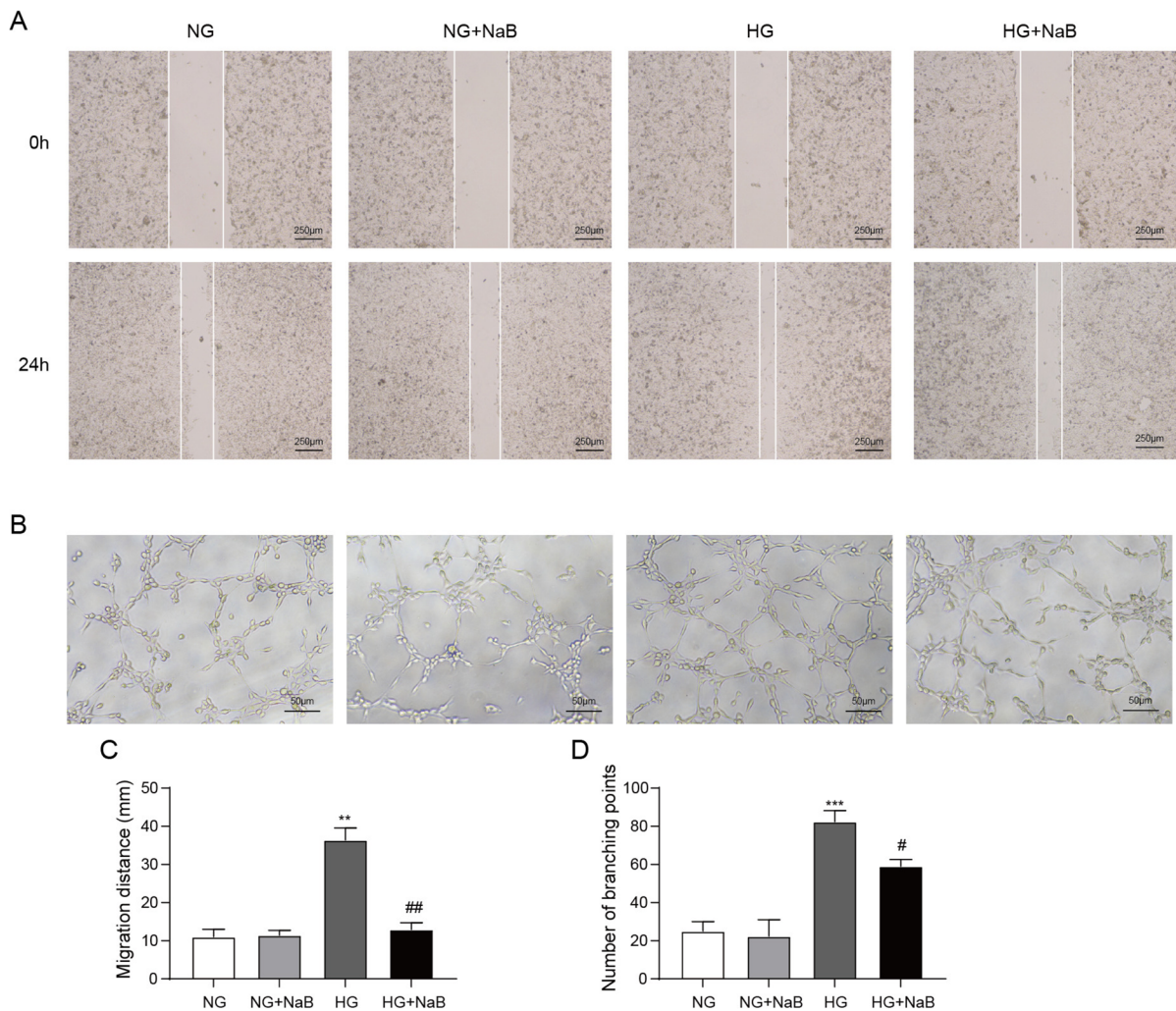


Fig. 5 Cell migration and tube formation affected by glucose and NaB in HRMECs. **A** Groups: (1) NG: normal glucose, 5.5 mM D-glucose; (2) NG+NaB: 5.5 mM D-glucose+5 mM NaB; (3) HG: 30 mM D-glucose; (4) HG+NaB: 30 mM D-glucose+5 mM NaB. Cell migration distance in HRMECs after scratched for 24 h with NG, NG+NaB, HG, HG+NaB administration. **B** Tube formation in HRMECs after

NG, NG+NaB, HG, HG+NaB administration. **C** Quantitative analysis of the cell migration distance of scratch test. **D** Quantitative analysis of the number of branching points of tube formation. ** $P < 0.01$ and *** $P < 0.001$ compared with the NG group; # $P < 0.05$, ## $P < 0.01$ compared with the HG group. Each experiment was repeated at least three times

as a novel therapeutic and protective strategy for addressing DR.

The buildup of ROS caused by hyperglycemia is linked to mitochondrial malfunction, local inflammation, cell death, and microvascular dysfunction. Overproduction of ROS, cell death, and local inflammation are all intimately related and have a significant influence on all stages of DR pathogenesis³⁵. The elevated production of pro-inflammatory cytokines and free radicals, coupled with processes

like leukocytosis, or the leukocyte adherence to retinal capillaries, contribute to amplified vascular permeability, loss of capillary pericyte, and the disruption of the blood retina barrier (BRB). Adhesion molecule (ICAM-1 and VCAM-1) and leukocyte activation increases are linked to DR development³⁷. Our study demonstrated that exposure to HG substantially increased the generation of ROS and inflammatory cytokines, as well as enhanced cell migration in HRMECs. Concurrently, NaB exhibited multifaceted

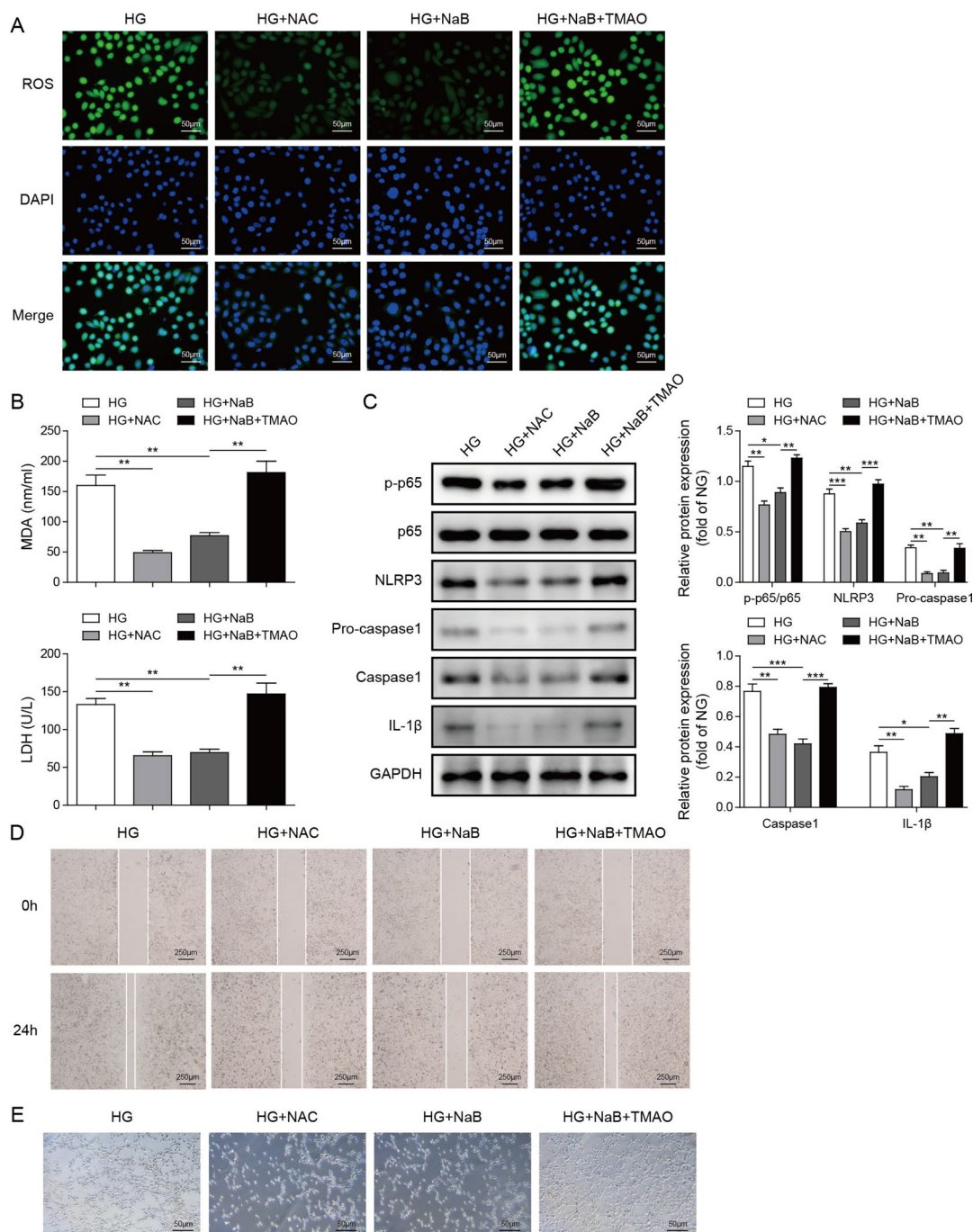


Fig. 6 Activation of ROS/NF- κ B/NLRP3 pathway and angiogenesis affected by glucose and NaB in HRMECs. Groups: (1) HG: 30 mM D-glucose; (2) HG + N-Acetyl-cysteine (NAC, ROS inhibitor): 30 mM D-glucose + 5 mM NAC; (3) HG + NaB: 30 mM D-glucose + 5 mM NaB; (4) HG + NaB + Trimethylamine N-oxide (TMAO, ROS activator): 30 mM D-glucose + 5 mM NaB + 5 mM TMAO. **A** Immuno-

fluorescence detection of cellular ROS levels. **B** Measurement of MDA and LDH levels. **C** Western blot analysis of NLRP3/NF- κ B pathways, caspase-1, and IL-1 β expression levels. **D** Scratch assay to assess cell migration. **E** In vitro angiogenesis assay to evaluate angiogenesis. * $P < 0.05$; ** $P < 0.01$; *** $P < 0.001$. Each experiment was repeated at least three times

biological effects, influencing cell signaling pathways via HDAC inhibition, modulation of mitochondrial activity, and interactions with G-protein coupled receptors (GPCRs) [41]. Edenil et al. conducted a study in which EA. hy926 cells were pretreated with butyrate (0.5 mM) two hours prior to exposure to oxidized low-density lipoprotein (oxLDL). The aim was to investigate the influence of butyrate pretreatment on endothelial cells. The results of their study indicated that endothelial cells pretreated with butyrate exhibited reduced levels of superoxide ion, hydrogen peroxide, and nitric oxide in response to oxLDL challenge [1]. Oral butyrate and inulin supplementation substantially boosted SOD activity in type 2 diabetes, according to Neda Roshanravan et al. SOD levels that are high may boost cellular defense against superoxide and peroxynitrite anions [24]. In our study, NaB significantly abrogated HG-induced oxidative stress of HRMECs. As for one phenomenon observed in our study that an increase in HRMECs cell viability under HG condition, which may indicate that the cells undergo adaptive changes when faced with a high glucose environment. High glucose conditions typically increase intracellular glucose metabolites, which may trigger the activation of various intracellular signaling pathways that could protect cell growth and survival [27]. Our experimental results show that HRMECs cell viability increases under high glucose conditions, possibly due to adaptive mechanisms in high glucose environments, such as enhanced antioxidant capacity or activation of repair mechanisms. This adaptive response may be a way for the cells to maintain their physiological functions [40].

The joint upstream event to remodel all four classical pathogenetic pathways of DR is always thought to be hyperglycemia-induced ROS production [7]. Prior research has suggested that the excessive generation of ROS plays a pivotal role in the activation of the NLRP3 inflammasome [32]. We had confirmed NaB reduced ROS generation, so we further studied if NaB has any effect on NF- κ B/NLRP3 pathway. Gu et al. showed that treatment with 5 mM NaB resulted in the reduction of increased IL-1 β secretion in the supernatant of mesangial cells induced by LPS or HG stimulation. Additionally, they observed that NaB inhibited the activation of the NF- κ B/I κ B- α signaling pathway in glomerular endothelial cells exposed to high glucose conditions [9]. Jiang et al. found that sodium butyrate might help prevent cow mastitis by relieving

LPS-induced series of inflammatory responses in bovine macrophages via inhibiting histone deacetylation and the canonical NF- κ B, NLRP3 signaling pathway [10]. In this study, we aimed to investigate the effect of NaB on the NF- κ B/NLRP3 pathway in HRMECs exposed to HG conditions. Our results indicate that NaB effectively decreased the activation of the NF- κ B/NLRP3 pathway induced by HG in HRMECs.

NPDR, the early stage of DR, is featured by increased retinal blood vessel permeability owing to the breakdown of BRB. The BRB is composed of both an inner and an outer barrier. The inner BRB is formed by tight junctions (TJ) between retinal capillary endothelial cells, while the outer BRB is composed of tight junctions between retinal pigment epithelial cells. The main inner and outer BRB TJ proteins were built on occludins, ZO proteins, claudins, and junctional adhesion molecules (JAMs) together [3]. Indeed, ZO-1, occludin, claudin-1, and claudin-5 are among the key TJ proteins that contribute to maintaining the integrity of the BRB [38]. Studies have indicated that HG can lead to a reduction in ZO-1 and occludin protein levels in retinal endothelial cells [11], and we got the same result in HG-induced HRMECs. Sodium butyrate improved the gastrointestinal barrier and the blood–brain barrier by upregulation of occludin and ZO-1 [8]. We found in our study that 5 mM NaB reversed the decrease in ZO-1 expression induced by HG in HRMECs.

N-Acetylcysteine (NAC), abbreviated as NAC, is an amino acid derivative known for its capacity as an antioxidant to diminish oxidative stress within cells [28]. By elevating the levels of glutathione (GSH), it aids cells in defending against damage caused by free radicals and oxidative molecules, thereby shielding cells from the impacts of oxidative stress [21]. Due to its antioxidative properties, NAC has been investigated for potential therapeutic applications in diseases such as cardiovascular ailments, neurological disorders, and inflammatory conditions [23]. Research suggests that utilizing NAC to reduce oxidative stress may offer assistance in managing and treating DR [31]. Trimethylamine N-oxide (TMAO) is a metabolite generated by gut microbiota, typically originating from certain nutrients in food such as choline and L-carnitine found in meats. These substances are metabolized by gut microbes to produce

trimethylamine (TMA), which is then oxidized into TMAO in the liver [42]. TMAO is believed to be associated with inflammation and oxidative stress, potentially affecting vascular homeostasis by activating inflammatory pathways and influencing the balance of oxidation–reduction [30]. Therefore, this study aims to investigate the impact of NaB on the ROS/NF- κ B/NLRP3 pathway using ROS inhibitor NAC and ROS activator TMAO, further exploring alterations in the migratory capacity and vascular formation ability of HRMECs. And we found that NaB inhibited HG-induced activation of ROS/NF- κ B/NLRP3 pathway and angiogenesis in HRMECs, which can be a new treatment for DR. However, we need further follow-up animal experiments on DR to validate the drug's safety and effectiveness in vivo.

In conclusion, our studies showed that NaB holds the potential to attenuate the activation of the ROS/NF- κ B/NLRP3 pathway and angiogenesis in HRMECs, indicating that NaB can be a new therapeutic and protective approach for DR. Our study provides new ideas for DR prevention and treatment. And what's more, in vivo and clinical trials will be further refined in future.

Acknowledgements We would like to give our sincere gratitude to the reviewers for their constructive comments.

Author contributions Xin Cao: Conceptualization, Methodology, Supervision, Writing—Original draft preparation, Investigation, Writing—Reviewing and Editing. Yue Di: Formal analysis, Methodology, Writing—Reviewing and Editing. Ya-Jing Tian: Investigation, Resources, Software. Xiao-Bo Huang: Resources, Data curation, Visualization. Yue Zhou: Validation, Visualization. Dong-Mei Zhang: Data curation, Formal analysis. Yu Song: Conceptualization, Supervision, Writing—Original draft preparation, Writing—Reviewing and Editing.

Funding General Program of Jiangsu Commission of Health (No. M2024093) and Natural Science Foundation (Youth Fund) of Science and Technology Bureau of Nantong City (No. JC2023028).

Availability of data and material All the data generated or analyzed during this study have been included in the article. Additionally, the datasets used or analyzed during the current study are available from the corresponding author upon reasonable request.

Declarations

Conflict of interest The authors declare that there was no conflict of interest.

Ethical approval Not applicable.

Consent for publication Not applicable.

Human or animal rights The article in question does not involve any studies conducted on human participants or animals by the authors.

References

1. Aguilar EC, Santos LC, Leonel AJ, de Oliveira JS, Santos EA, Navia-Pelaez JM, da Silva JF, Mendes BP, Capettini LS, Teixeira LG, Lemos VS, Alvarez-Leite JI (2016) Oral butyrate reduces oxidative stress in atherosclerotic lesion sites by a mechanism involving NADPH oxidase down-regulation in endothelial cells. *J Nutr Biochem* 34:99–105
2. Alsoudi AF, Wai KM, Koo E, Parikh R, Mruthunjaya P, Rahimy E (2024) Initial therapy of panretinal photocoagulation vs anti-VEGF injection for proliferative diabetic retinopathy. *JAMA Ophthalmol* 142:947
3. Antonetti DA, Silva PS, Stitt AW (2021) Current understanding of the molecular and cellular pathology of diabetic retinopathy. *Nat Rev Endocrinol* 17:195–206
4. Chen W, Zhao M, Zhao S, Lu Q, Ni L, Zou C, Lu L, Xu X, Guan H, Zheng Z, Qiu Q (2017) Activation of the TXNIP/NLRP3 inflammasome pathway contributes to inflammation in diabetic retinopathy: a novel inhibitory effect of minocycline. *Inflamm Res* 66:157–166
5. Chen X, Kong Q, Zhao X, Zhao C, Hao P, Irshad I, Lei H, Kulyar MF, Bhutta ZA, Ashfaq H, Sha Q, Li K, Wu Y (2022) Sodium acetate/sodium butyrate alleviates lipopolysaccharide-induced diarrhea in mice via regulating the gut microbiota, inflammatory cytokines, antioxidant levels, and NLRP3/Caspase-1 signaling. *Front Microbiol* 13:1036042
6. Du Y, Tang G, Yuan W (2020) Suppression of HDAC2 by sodium butyrate alleviates apoptosis of kidney cells in db/db mice and HG-induced NRK-52E cells. *Int J Mol Med* 45:210–222
7. Forbes JM, Coughlan MT, Cooper ME (2008) Oxidative stress as a major culprit in kidney disease in diabetes. *Diabetes* 57:1446–1454
8. Fu J, Li G, Wu X, Zang B (2019) Sodium butyrate ameliorates intestinal injury and improves survival in a rat model of cecal ligation and puncture-induced sepsis. *Inflammation* 42:1276–1286
9. Gu J, Huang W, Zhang W, Zhao T, Gao C, Gan W, Rao M, Chen Q, Guo M, Xu Y, Xu YH (2019) Sodium butyrate alleviates high-glucose-induced renal glomerular endothelial cells damage via inhibiting pyroptosis. *Int Immunopharmacol* 75:105832
10. Jiang L, Wang J, Liu Z, Jiang A, Li S, Wu D, Zhang Y, Zhu X, Zhou E, Wei Z, Yang Z (2020) Sodium butyrate alleviates lipopolysaccharide-induced inflammatory responses by down-regulation of NF- κ B, NLRP3 signaling pathway, and activating histone acetylation in bovine macrophages. *Front Vet Sci* 7:579674
11. Jiang Y, Liu L, Steinle JJ (2017) Compound 49b regulates ZO-1 and occludin levels in human retinal

- endothelial cells and in mouse retinal vasculature. *Invest Ophthalmol Vis Sci* 58:185–189
12. Khan S, Jena GB (2014) Protective role of sodium butyrate, a HDAC inhibitor on beta-cell proliferation, function and glucose homeostasis through modulation of p38/ERK MAPK and apoptotic pathways: study in juvenile diabetic rat. *Chem Biol Interact* 213:1–12
 13. Lee HJ, Son Y, Lee M, Moon C, Kim SH, Shin IS, Yang M, Bae S, Kim JS (2019) Sodium butyrate prevents radiation-induced cognitive impairment by restoring pCREB/BDNF expression. *Neural Regen Res* 14:1530–1535
 14. Li H, Gao Z, Zhang J, Ye X, Xu A, Ye J, Jia W (2012) Sodium butyrate stimulates expression of fibroblast growth factor 21 in liver by inhibition of histone deacetylase 3. *Diabetes* 61:797–806
 15. Li J, Lu X, Wei L, Ye D, Lin J, Tang X, Cui K, Yu S, Xu Y, Liang X (2022) PHD2 attenuates high-glucose-induced blood retinal barrier breakdown in human retinal microvascular endothelial cells by regulating the Hif-1 α /VEGF pathway. *Inflamm Res* 71:69–79
 16. Li Y, Busoy JM, Zaman BAA, Tan QSW, Tan GSW, Barathi VA, Cheung N, Wei JJ, Hunziker W, Hong W, Wong TY, Cheung CMG (2018) A novel model of persistent retinal neovascularization for the development of sustained anti-VEGF therapies. *Exp Eye Res* 174:98–106
 17. Luo QJ, Sun MX, Guo YW, Tan SW, Wu XY, Abassa KK, Lin L, Liu HL, Jiang J, Wei XQ (2021) Sodium butyrate protects against lipopolysaccharide-induced liver injury partially via the GPR43/ β -arrestin-2/NF- κ B network. *Gastroenterol Rep (Oxf)* 9:154–165
 18. Ma X, Zhou Z, Zhang X, Fan M, Hong Y, Feng Y, Dong Q, Diao H, Wang G (2020) Sodium butyrate modulates gut microbiota and immune response in colorectal cancer liver metastatic mice. *Cell Biol Toxicol* 36:509–515
 19. Masters SL, Latz E, O'Neill LA (2011) The inflammatory in atherosclerosis and type 2 diabetes. *Sci Transl Med* 3:81ps17
 20. Mittal M, Siddiqui MR, Tran K, Reddy SP, Malik AB (2014) Reactive oxygen species in inflammation and tissue injury. *Antioxid Redox Signal* 20:1126–1167
 21. Pedre B, Barayeu U, Ezeriņa D, Dick TP (2021) The mechanism of action of N-acetylcysteine (NAC): the emerging role of H(2)S and sulfane sulfur species. *Pharmacol Ther* 228:107916
 22. Pietrzak A, Banasiuk M, Szczepanik M, Borys-Iwanicka A, Pytrus T, Walkowiak J, Banaszkiewicz A (2022) Sodium butyrate effectiveness in children and adolescents with newly diagnosed inflammatory bowel diseases-randomized placebo-controlled multicenter trial. *Nutrients* 14:3283
 23. Raghu G, Berk M, Campochiaro PA, Jaeschke H, Marenzi G, Richeldi L, Wen FQ, Nicoletti F, Calverley PMA (2021) The multifaceted therapeutic role of n-acetylcysteine (NAC) in disorders characterized by oxidative stress. *Curr Neuropharmacol* 19:1202–1224
 24. Roshanravan N, Alamdari NM, Jafarabadi MA, Mohammadi A, Shabestari BR, Nasirzadeh N, Asghari S, Mansoori B, Akbarzadeh M, Ghavami A, Ghaffari S, Ostadrahimi A (2020) Effects of oral butyrate and inulin supplementation on inflammation-induced pyroptosis pathway in type 2 diabetes: a randomized, double-blind, placebo-controlled trial. *Cytokine* 131:155101
 25. Sabanayagam C, Banu R, Chee ML, Lee R, Wang YX, Tan G, Jonas JB, Lamoureux EL, Cheng CY, Klein BEK, Mitchell P, Klein R, Cheung CMG, Wong TY (2019) Incidence and progression of diabetic retinopathy: a systematic review. *Lancet Diabetes Endocrinol* 7:140–149
 26. Santiago AR, Boia R, Aires ID, Ambrósio AF, Fernandes R (2018) Sweet stress: coping with vascular dysfunction in diabetic retinopathy. *Front Physiol* 9:820
 27. Serikbaeva A, Li Y, Ganesh B, Zelkha R, Kazlauskas A (2022) Hyperglycemia promotes mitophagy and thereby mitigates hyperglycemia-induced damage. *Am J Pathol* 192:1779–1794
 28. Tenório M, Graciliano NG, Moura FA, Oliveira ACM, Goulart MOF (2021) N-acetylcysteine (NAC): impacts on human health. *Antioxidants (Basel)* 10:967
 29. Teo ZL, Tham YC, Yu M, Chee ML, Rim TH, Cheung N, Bikbov MM, Wang YX, Tang Y, Lu Y, Wong IY, Ting DSW, Tan GSW, Jonas JB, Sabanayagam C, Wong TY, Cheng CY (2021) Global prevalence of diabetic retinopathy and projection of burden through 2045: systematic review and meta-analysis. *Ophthalmology* 128:1580–1591
 30. Thomas MS, Fernandez ML (2021) Trimethylamine N-oxide (TMAO), diet and cardiovascular disease. *Curr Atheroscler Rep* 23:12
 31. Tosi GM, Giustarini D, Franci L, Minetti A, Imperatore F, Caldi E, Fiorenzani P, Aloisi AM, Sparatore A, Rossi R, Chiariello M, Orlandini M, Galvagni F (2021) Superior properties of N-acetylcysteine ethyl ester over N-acetyl cysteine to prevent retinal pigment epithelial cells oxidative damage. *Int J Mol Sci* 22:600
 32. Wang F, Liang Q, Ma Y, Sun M, Li T, Lin L, Sun Z, Duan J (2022) Silica nanoparticles induce pyroptosis and cardiac hypertrophy via ROS/NLRP3/Caspase-1 pathway. *Free Radic Biol Med* 182:171–181
 33. Wang X, He G, Peng Y, Zhong W, Wang Y, Zhang B (2015) Sodium butyrate alleviates adipocyte inflammation by inhibiting NLRP3 pathway. *Sci Rep* 5:12676
 34. Wei H, Gu Q (2022) SOX4 promotes high-glucose-induced inflammation and angiogenesis of retinal endothelial cells by activating NF- κ B signaling pathway. *Open Life Sci* 17:393–400
 35. Wu MY, Yiang GT, Lai TT, Li CJ (2018) The oxidative stress and mitochondrial dysfunction during the pathogenesis of diabetic retinopathy. *Oxid Med Cell Longev* 2018:3420187
 36. Xiao X, Chen M, Xu Y, Huang S, Liang J, Cao Y, Chen H (2020) Sodium Butyrate Inhibits Neovascularization Partially via TNXIP/VEGFR2 Pathway. *Oxid Med Cell Longev* 2020:6415671
 37. Yao Y, Du J, Li R, Zhao L, Luo N, Zhai JY, Long L (2019) Association between ICAM-1 level and diabetic retinopathy: a review and meta-analysis. *Postgrad Med J* 95:162–168
 38. Yu S, Cui K, Wu P, Wu B, Lu X, Huang R, Tang X, Lin J, Yang B, Zhao J, He Q, Liang X, Xu Y (2022) Melatonin prevents experimental central serous chorioretinopathy in rats. *J Pineal Res* 73:e12802
 39. Yuan X, Wang L, Bhat OM, Lohner H, Li PL (2018) Differential effects of short chain fatty acids on endothelial

- Nlrp3 inflammasome activation and neointima formation: antioxidant action of butyrate. *Redox Biol* 16:21–31
40. Zhang D, Jin W, Wu R, Li J, Park SA, Tu E, Zanvit P, Xu J, Liu O, Cain A, Chen W (2019) High glucose intake exacerbates autoimmunity through reactive-oxygen-species-mediated TGF- β cytokine activation. *Immunity* 51:671–681.e5
 41. Zhang N, Qin B (2021) Research progress of sodium butyrate in metabolic-associated fatty liver disease. *Zhonghua Gan Zang Bing Za Zhi* 29:1229–1232
 42. Zhu W, Romano KA, Li L, Buffa JA, Sangwan N, Prakash P, Tittle AN, Li XS, Fu X, Androjna C, DiDonato AJ, Brinson K, Trapp BD, Fischbach MA, Rey FE, Hajjar AM, DiDonato JA, Hazen SL (2021) Gut microbes impact

stroke severity via the trimethylamine N-oxide pathway. *Cell Host Microbe* 29:1199–1208.e5

Publisher's Note Springer Nature remains neutral with regard to jurisdictional claims in published maps and institutional affiliations.

Springer Nature or its licensor (e.g. a society or other partner) holds exclusive rights to this article under a publishing agreement with the author(s) or other rightsholder(s); author self-archiving of the accepted manuscript version of this article is solely governed by the terms of such publishing agreement and applicable law.